

# Data-driven Morozov regularization of inverse problems

Markus Haltmeier\*, Richard Kowar, and Markus Tiefenthaler

Department of Mathematics, University of Innsbruck  
Technikerstrasse 13, 6020 Innsbruck, Austria

October 21, 2024

## Abstract

The solution of inverse problems is crucial in various fields such as medicine, biology, and engineering, where one seeks to find a solution from noisy observations. These problems often exhibit non-uniqueness and ill-posedness, resulting in instability under noise with standard methods. To address this, regularization techniques have been developed to balance data fitting and prior information. Recently, data-driven variational regularization methods have emerged, mainly analyzed within the framework of Tikhonov regularization, termed Network Tikhonov (NETT). This paper introduces Morozov regularization combined with a learned regularizer, termed DD-Morozov regularization. Our approach employs neural networks to define non-convex regularizers tailored to training data, enabling a convergence analysis in the non-convex context with noise-dependent regularizers. We also propose a refined training strategy that improves adaptation to ill-posed problems compared to NETT's original strategy, which primarily focuses on addressing non-uniqueness. We present numerical results for attenuation correction in photoacoustic tomography, comparing DD-Morozov regularization with NETT using the same trained regularizer, both with and without an additional total variation regularizer.

**Key words:** Inverse problems, learned regularizer, convergence analysis, Morozov regularization, neural networks.

**MSC codes:** 65F22; 68T07

## 1 Introduction

In this paper, we consider the solution of linear inverse problems where we aim to reconstruct the unknown  $x \in \mathbb{X}$  from noisy data

$$y_\delta = \mathbf{A}x + \eta_\delta. \tag{1.1}$$

---

\*Corresponding author: [markus.haltmeier@uibk.ac.at](mailto:markus.haltmeier@uibk.ac.at)

Here  $\mathbf{A}: \mathbb{X} \rightarrow \mathbb{Y}$  is a linear bounded operator between Hilbert spaces  $\mathbb{X}$  and  $\mathbb{Y}$ , and  $\eta_\delta$  is the data error that satisfies  $\|\eta_\delta\| \leq \delta$  with noise level  $\delta \geq 0$ . We are especially interested in the ill-posed case where solving (1.1) without prior information is non-unique or unstable. After discretization, this leads to linear systems of equations with perturbed right hand side and a forward matrix that possesses a large kernel, many small singular values, or both. Several applications in medical image reconstruction, nondestructive testing, and remote sensing are instances of such linear inverse problems [15, 41, 49].

Characteristic features of inverse problems are the non-uniqueness of solutions and the unstable dependence of solutions on data perturbations. To account for these two issues, one must apply regularization methods (see, for example, [8, 15, 22, 26, 27, 37, 49, 50, 52]) that serve two main purposes: First, in the case of exact data  $y \in \text{ran}(\mathbf{A})$ , they select a specific solution  $\mathbf{B}_0(y)$  among all possible solutions of the exact data equation  $y = \mathbf{A}x$ . Second, to account for noise, they define stable approximations to  $\mathbf{B}_0$  in the form of continuous mappings  $\mathbf{B}_\alpha: \mathbb{Y} \rightarrow \mathbb{X}$  that converge to  $\mathbf{B}_0$  as  $\alpha \rightarrow 0$  in an appropriate sense.

## 1.1 Morozov regularization

There are several well established methods for the stable solution of inverse problems. A general class of regularization methods are variational regularization methods which includes Tikhonov regularization, Ivanov regularization (the method of quasi solutions), and Morozov regularization (the residual method) as special cases. In Tikhonov regularization, approximate solutions are defined as minimizers of  $\|\mathbf{A}x - y_\delta\|^2/2 + \alpha\mathcal{R}(x)$ , where  $\mathcal{R}: \mathbb{X} \rightarrow [0, \infty]$  is a regularization functional that measures the feasibility of a potential solution and  $\alpha$  is the regularization parameter. Ivanov regularization considers minimizers of  $\|\mathbf{A}x - y_\delta\|$  over the set  $\{x \in \mathbb{X} \mid \mathcal{R}(x) \leq \tau\}$  for some  $\tau > 0$ . In this paper, we consider Morozov regularization where approximate solutions defined as solutions of

$$\min_{x \in \mathbb{X}} \mathcal{R}(x) \quad \text{s.t.} \quad \|\mathbf{A}x - y_\delta\| \leq \delta. \quad (1.2)$$

Compared to Tikhonov regularization and Ivanov regularization, the latter has the advantage that no additional regularization parameter has to be selected, which is typically a difficult issue. Relations between Tikhonov regularization, Ivanov regularization and Morozov regularization are carefully studied in [27]. A general convergence analysis of Morozov regularization, including convergence rates, has been carried out in [20].

Note that variational regularization methods are designed to approximate  $\mathcal{R}$ -minimizing solution of  $\mathbf{A}x = y$  for the limit  $\delta \rightarrow 0$ , defined as elements in  $\arg \min\{\mathcal{R}(x) \mid \mathbf{A}x = y\}$ . This addresses the non-uniqueness in the case of exact data. To account for noisy data  $y_\delta$ , Morozov regularization relaxes the strict data consistency  $\mathbf{A}x = y$  to data proximity  $\|\mathbf{A}x - y_\delta\| \leq \delta$ .

Even in the case that  $\mathbf{A}$  is injective, different regularization terms behave differently and significantly affect convergence. Therefore the choice of the regularizer is crucial and a nontrivial issue. Classical choices for the regularizers are the squared Hilbert space norm  $\mathcal{R}(x) = \|x\|^2/2$  or the  $\ell^1$ -norm  $\mathcal{R}(x) = \sum_{\lambda \in \Lambda} |\langle u_\lambda, x \rangle|$ , where  $(u_\lambda)_\lambda$  is a frame of  $\mathbb{X}$ . These regularizers may not be optimally adapted to highly structured signal classes, as is often the case in practical applications. In this paper, we address this issue and propose a data-driven regularizer using neural networks adapted to the signal class represented by training data in combination with Morozov regularization.

## 1.2 Neural network regularizers

In this paper, we study Morozov regularization with a neural network based, data-driven and noise-level-dependent regularizer

$$\mathcal{R}_\delta(x) = \frac{1}{2} \|\Phi_{\theta(\delta)}(x) - x\|^2 + \lambda \mathcal{Q}(x). \quad (1.3)$$

Here  $\Phi_{\theta(\delta)}: \mathbb{X} \rightarrow \mathbb{X}$  is a neural network tuned to noisy data, and  $\mathcal{Q}: \mathbb{X} \rightarrow [0, \infty]$  is an additional regularization term. While  $\mathcal{Q}$  is mainly added for theoretical purposes to guarantee coercivity, in the numerical results we show that it also has a beneficial influence on the reconstruction. For the theoretical analysis the squared Hilbert space norm  $\mathcal{Q} = \|\cdot\|^2$  would be sufficient. We refer to (1.2) with the data-driven regularizer (1.3) instead of the fixed regularizer  $\mathcal{R}$  as data-driven Morozov (DD-Morozov) regularization. We will show that, under reasonable assumptions, the latter provides a convergent regularization method. Furthermore, we present a training strategy for selecting the noise-dependent neural network for a given architecture. Note that a noise-level-independent network is also included in our analysis. Allowing the networks to depend on  $\delta$ , however, enables the networks to better adapt to available noisy training data.

Besides stabilizing the signal reconstruction, the main purpose of a particular regularizer is to fit the reconstructions to a certain set where the true signals are likely to be contained. In reality, this set is not known analytically, but it is possible to draw examples from it. For this reason, we follow the learning paradigm and choose training signals  $x_1, \dots, x_N \in \mathbb{X}$  and adapt the architecture  $(\Phi_\theta)_{\theta \in \Theta}$  to  $x_i$  and corresponding noisy measurements. More precisely,  $\theta = \theta(\delta)$  is chosen such that  $\Phi_\theta(x_i) \simeq x_i$  and  $\Phi_\theta(x_i + r_{i,j}) \simeq x_i$ , where  $r_{i,j}$  are certain perturbations that are allowed to depend on the forward operator and on the noise. Thus,  $\mathcal{R}_\delta$  has small values for the exact  $x_i$  and larger values for the perturbed signals  $x_i + r_{i,j}$ . Since the training signals  $x_i$  are only taken from a certain potentially small subset of  $\mathbb{X}$ , it is difficult to obtain the necessary coercive condition from training alone. Therefore, it seems natural to add another regularization term  $\mathcal{Q}$  which is known to be coercive.

In Section 2.2 we propose a possible choice for the perturbations  $r_{i,j}$  resulting in a novel training strategy for the regularizer. This refines the training strategy of the NETT paper [35] and seems more suitable for ill-posed and ill-conditioned problems. In the original NETT strategy, all added perturbations are in the null space of the forward operator, and the task of the learned regularizer was purely the selection of a proper solution in the limit. The refined training strategy refers to the added perturbations  $r_{i,j}$  that might have components outside the null space of the forward operator. In the case of several small singular values the proposed regularizer can correct for signal components damped by small singular values with an amount determined by the noise level.

While learned regularizers have recently become popular in the context of Tikhonov regularization [19, 35, 36, 42], we are not aware of any work utilizing the Morozov variant. In fact, our analysis as well as the training strategy are related to the Network Tikhonov Approach (NETT) of [35, 42]. A very different strategy for learning a network regularizer has been proposed in [36] in the context of adversarial regularization. Other approaches for learning a regularizer are the fields of experts model [48], deep total variation [28] or ridge regularizers [19]. Other data-driven regularization methods for inverse problems can be found for example in [3, 5, 6, 12, 22, 38, 45, 51] and the references therein. From the theoretical side, Morozov regularization in a general non-convex context has been studied in [20]. The analysis we present below allows the regularizer to be noise-dependent and further we derive strong convergence under total nonlinearity condition of [35].

### 1.3 Outline

The remainder of this paper is organized as follows. In Section 2 we present our theoretical results. In particular we present the convergence analysis (Section 2.1) and the proposed training strategy (Section 2.2). In Section 3 we present numerical results illustrating DD-Morozov regularization with and without TV as additional regularizer. Specifically, we test our approach on an inverse problem for one-dimensional attenuation correction in photoacoustic tomography in damping media [30] and compare DD-Morozov regularization with and without TV to NETT regularization and pure TV regularization. To numerically solve (1.2) we implement the primal dual scheme of [10]. The paper concludes with a short summary in Section 4.

## 2 Theory

Throughout this paper,  $\mathbb{X}$ ,  $\mathbb{Y}$  are Hilbert spaces and  $\mathbf{A}: \mathbb{X} \rightarrow \mathbb{Y}$  a bounded linear operator with potentially non-trivial nullspace. Recall that a functional  $\mathcal{R}: \mathbb{X} \rightarrow [0, \infty]$  is coercive, if  $\mathcal{R}(x_n) \rightarrow \infty$  for all sequences  $(x_n)_{n \in \mathbb{N}} \in \mathbb{X}^{\mathbb{N}}$  with  $\|x_n\|_{\mathbb{X}} \rightarrow \infty$ , and weakly lower semicontinuous, if  $\mathcal{R}(x) \leq \liminf_{n \rightarrow \infty} \mathcal{R}(x_n)$  for  $(x_n)_{n \in \mathbb{N}} \rightharpoonup x$ , where  $\rightharpoonup$  denotes weak convergence, and

→ strong convergence. Any element in  $\arg \min \{\mathcal{R}(x) \mid \mathbf{A}x = y\}$  is called an  $\mathcal{R}$ -minimizing solution of the equation  $\mathbf{A}x = y$ .

## 2.1 Convergence analysis

For neural networks  $\Phi, \Phi_{\theta(\delta)}$  on  $\mathbb{X}$  and noise level  $\delta > 0$  we define the noise-dependent regularizer  $\mathcal{R}_\delta$  by (1.3), the limiting regularizer by  $\mathcal{R}(x) = \|\Phi(x) - x\|^2/2 + \lambda \mathcal{Q}(x)$  and consider DD-Morozov regularization

$$\min_{x \in \mathbb{X}} \mathcal{R}_\delta(x) \quad \text{s.t.} \quad \|\mathbf{A}x - y_\delta\| \leq \delta. \quad (2.1)$$

Our results on the convergence of (1.3), (2.1) are derived under the following conditions, which we assume to be satisfied throughout this subsection.

### Assumption 2.1.

- (A1)  $\Phi, \Phi_{\theta(\delta)}: \mathbb{X} \rightarrow \mathbb{X}$  are weakly continuous.
- (A2)  $\Phi_{\theta(\delta)} \rightarrow \Phi$  weakly uniformly on bounded sets as  $\delta \rightarrow 0$ .
- (A3)  $\Phi_{\theta(\delta)} \rightarrow \Phi$  strongly pointwise on  $\mathcal{R}$ -minimizing solutions as  $\delta \rightarrow 0$ .
- (A4)  $\mathcal{Q}: \mathbb{X} \rightarrow [0, \infty]$  is proper, coercive and weakly lower semicontinuous.

In (A2), weak uniform convergence on bounded sets means that for all bounded  $B \subseteq \mathbb{X}$  and all  $h \in \mathbb{X}$  we have  $\sup_{x \in B} |\langle \Phi_{\theta(\delta)}(x) - \Phi(x), h \rangle| = 0$  as  $\delta \rightarrow 0$ . In the convergence analysis we assume that the networks  $\Phi_{\theta(\delta)}$  are trained, where  $\theta(\delta)$  potentially depends on the noise level, and that the forward operator  $\mathbf{A}$  and the additional regularizer  $\mathcal{Q}$  are given by the application or are user-specified. In many applications,  $\|(\Phi_{\theta(\delta)} - \text{Id})(\cdot)\|$  may not be coercive which is the reason to add the term  $\mathcal{Q}$  in (1.3).

**Lemma 2.2.** *The regularizers  $\mathcal{R}, \mathcal{R}_\delta$  are coercive and weakly sequentially lower semicontinuous. Further, the feasible set  $\{x \in \mathbb{X} \mid \|\mathbf{A}x - y_\delta\| \leq \delta\}$  is weakly closed and non-empty for all  $\delta > 0$  and all data  $y_\delta$  with  $\|\mathbf{A}x_\star - y_\delta\| \leq \delta$  for some  $x_\star \in \text{dom}(\mathcal{Q})$ .*

*Proof.* Let  $(x_n)_{n \in \mathbb{N}} \in \mathbb{X}^{\mathbb{N}}$ . Because  $\mathcal{Q}$  is coercive and  $\|\Phi(x) - x\|^2, \|\Phi_{\theta(\delta)}(x) - x\|^2$  are non-negative, the functionals  $\mathcal{R}, \mathcal{R}_\delta$  are coercive. Let  $(x_n)_{n \in \mathbb{N}} \in \mathbb{X}^{\mathbb{N}}$  converge weakly to  $x \in \mathbb{X}$ . Because  $\Phi$  is weakly continuous,  $(\Phi(x_n) - x_n)_{n \in \mathbb{N}}$  converges weakly to  $\Phi(x) - x$ . Due to the weak sequential lower semicontinuity of the norm, we infer  $\|\Phi(x) - x\|_{\mathbb{X}} \leq \liminf_{n \rightarrow \infty} \|\Phi(x_n) - x_n\|_{\mathbb{X}}$  which shows that  $\mathcal{R}$  and in a similar manner  $\mathcal{R}_\delta$  are weakly lower semicontinuous. Now, according to [9, Lemma 1.2.3], a functional  $\mathcal{F}$  is weakly sequentially lower semicontinuous if and only if  $\{x \in \mathbb{X} \mid \mathcal{F}(x) \leq t\}$  is weakly sequentially closed for all  $t > 0$ . Because  $\mathbf{A}$  is linear and bounded it is weakly continuous. Because the norm is weakly sequentially lower

semicontinuous,  $x \mapsto \|\mathbf{A}x - y_\delta\|$  is weakly sequentially lower semicontinuous, too. Hence  $\{x \in \mathbb{X} \mid \|\mathbf{A}x - y_\delta\| \leq \delta\}$  is weakly closed for all  $\delta > 0$  and non-empty as it contains the exact data  $\mathbf{A}x_\star$ .  $\square$

**Lemma 2.3** (Existence). *For all data  $y_\delta \in \mathbb{Y}$  with  $\|\mathbf{A}x - y_\delta\| \leq \delta$  for some  $x \in \text{dom}(\mathcal{Q})$ , the constraint optimization problem (2.1) has at least one solution.*

*Proof.* Because  $\mathcal{R}_\delta \geq 0$ , the infimum  $M$  of  $\mathcal{R}$  over  $S_\delta := \{x \in \mathbb{X} \mid \|\mathbf{A}x - y_\delta\| \leq \delta\}$  is nonnegative and there exists a sequence  $(x_m)_m$  of elements of  $S_\delta$  with  $\lim_{m \rightarrow \infty} \mathcal{R}_\delta(x_m) = M$ . Because  $\mathcal{R}_\delta$  is coercive and  $\{\mathcal{R}_\delta(x_m) \mid m \in \mathbb{N}\}$  is bounded, we infer that  $(x_m)_m$  is bounded and thus there exists a weakly convergent subsequence  $(x_{m(k)})_k$  converging to some  $x \in \mathbb{X}$ . Moreover, due to the weak closedness of  $S_\delta$  we obtain  $x \in S_\delta$ . Because  $\mathcal{R}_\delta$  is weakly lower semicontinuous,  $\mathcal{R}(x) \leq M$  and thus  $x$  is a solution of (2.1).  $\square$

Analogous to the proof of Lemma 2.3 one shows that there exists at least one  $\mathcal{R}$ -minimizing solution of  $\mathbf{A}x = y$  whenever it is solvable in  $\text{dom}(\mathcal{Q})$ .

**Theorem 2.4** (Weak convergence). *Let  $\mathbf{A}x = y$  be solvable in  $\text{dom}(\mathcal{Q})$ ,  $(y_n)_{n \in \mathbb{N}} \in \mathbb{Y}^{\mathbb{N}}$  satisfy  $\|y - y_n\| \leq \delta_n$ , where  $(\delta_n)_{n \in \mathbb{N}} \in (0, \infty)^{\mathbb{N}}$  with  $\delta_n \rightarrow 0$ , write  $\mathcal{R}_n := \mathcal{R}_{\delta_n}$  and  $\Phi_n := \Phi_{\theta(\delta_n)}$ , and choose  $x_n \in \arg \min\{\mathcal{R}_n(z) \mid \|\mathbf{A}z - y_n\| \leq \delta_n\}$ . Then  $(x_n)_{n \in \mathbb{N}}$  has at least one weak accumulation point  $x^+ \in \mathbb{X}$ . Moreover, the limit of each weakly converging subsequence  $(x_{n(k)})_{k \in \mathbb{N}}$  is an  $\mathcal{R}$ -minimizing solution of  $\mathbf{A}x = y$  and  $\mathcal{R}_{n(k)}(x_{n(k)}) \rightarrow \mathcal{R}(x^+)$  for  $k \rightarrow \infty$ . If the  $\mathcal{R}$ -minimizing solution  $x^+$  of  $\mathbf{A}x = y$  is unique, then  $x_n \rightharpoonup x^+$  and  $\mathcal{R}_n(x_n) \rightarrow \mathcal{R}(x^+)$  as  $n \rightarrow \infty$ .*

*Proof.* Set  $S_n := \{z \in \mathbb{X} \mid \|\mathbf{A}z - y_n\| \leq \delta_n\}$  and  $S_\star := \{z \in \mathbb{X} \mid \mathbf{A}z = y\}$ . Clearly  $S_\star \subseteq S_n$  and because  $\mathbf{A}x = y$  is solvable,  $S_\star$  is non-empty. Thus  $\mathcal{Q}(x_n) + \|\Phi_n(x_n) - x_n\|^2/2 = \mathcal{R}_n(x_n) \leq \mathcal{R}_n(x_\star) = \mathcal{Q}(x_\star) + \|\Phi_n(x_\star) - x_\star\|^2/2$ , where  $x_\star$  is an  $\mathcal{R}$ -minimizing solution of  $\mathbf{A}x = y$ . From the weak convergence of  $\Phi_n(x_\star)$  we see that the right hand side is bounded. Thus  $\mathcal{Q}(x_n)$  is bounded and with the coercivity of  $\mathcal{Q}$  we conclude there exists a weakly converging subsequence  $(x_{n(k)})_{k \in \mathbb{N}}$ . Because  $\|\mathbf{A}(\cdot) - y\|$  is weakly lower semicontinuous,

$$\begin{aligned} \|\mathbf{A}(x^+) - y\| &\leq \liminf_{k \rightarrow \infty} \|\mathbf{A}(x_{n(k)}) - y\| \\ &\leq \liminf_{k \rightarrow \infty} \|\mathbf{A}(x_{n(k)}) - y_{n(k)}\| + \|y_{n(k)} - y\| \leq 2\delta_{n(k)} \end{aligned} \quad (2.2)$$

and thus  $x^+ \in S_\star$ . It remains to verify that  $x^+$  is an  $\mathcal{R}$ -minimizing solution of  $\mathbf{A}x = y$ . According to (A1), (A2) we have  $\Phi_{n(k)}(x_{n(k)}) \rightharpoonup \Phi(x^+)$  and  $\Phi_n(x_\star) \rightarrow \Phi(x_\star)$  as the weak uniform convergence assumption (A2) implies that for all bounded  $B \subseteq \mathbb{X}$  and all  $z \in \mathbb{X}$  we

have  $\sup_{x \in B} \langle \Phi_{n(k)}(x) - \Phi(x), z \rangle \rightarrow 0$ . Thus

$$\begin{aligned}
\mathcal{Q}(x^+) + \frac{\lambda}{2} \|\Phi(x^+) - x^+\| &\leq \liminf_{k \rightarrow \infty} \mathcal{Q}(x_{n(k)}) + \frac{\lambda}{2} \|\Phi_{n(k)}(x_{n(k)}) - x_{n(k)}\| \\
&\leq \limsup_{k \rightarrow \infty} \mathcal{Q}(x_{n(k)}) + \frac{\lambda}{2} \|\Phi_{n(k)}(x_{n(k)}) - x_{n(k)}\| \\
&\leq \limsup_{k \rightarrow \infty} \mathcal{Q}(x_*) + \frac{\lambda}{2} \|\Phi_{n(k)}(x_*) - x_*\| \\
&= \mathcal{Q}(x_*) + \frac{\lambda}{2} \|\Phi(x_*) - x_*\|.
\end{aligned}$$

Therefore  $x^+$  is an  $\mathcal{R}$ -minimizing solution of  $\mathbf{A}x = y$  with  $\mathcal{R}(x_{n(k)}) \rightarrow \mathcal{R}(x^+)$ . Finally, if the  $\mathcal{R}$ -minimizing solution  $x^+$  of  $\mathbf{A}x = y$  is unique, then  $(x_n)_{n \in \mathbb{N}}$  has exactly one weak accumulation point  $x^+$  and  $\mathcal{R}_n(x_n) \rightarrow \mathcal{R}(x^+)$ .  $\square$

Following [35], we introduce the concept of total nonlinearity, which is required for strong convergence.

**Definiton 2.5** (Total nonlinearity). *Let  $\mathcal{F}: \mathbb{X} \rightarrow \mathbb{R}$  be Gâteaux differentiable at  $x_* \in \mathbb{X}$ . The absolute Bregman distance  $\mathcal{B}_{\mathcal{F}}(x_*, \cdot): \mathbb{X} \rightarrow [0, \infty]$  and the modulus of total nonlinearity  $\nu_{\mathcal{F}}(x_*, \cdot): (0, \infty) \rightarrow [0, \infty]$  of  $\mathcal{F}$  at  $x_*$  are defined by*

$$\forall x \in \mathbb{X}: \quad \mathcal{B}_{\mathcal{F}}(x_*, x) := |\mathcal{F}(x) - \mathcal{F}(x_*) - \mathcal{F}'(x_*)(x - x_*)| \quad (2.3)$$

$$\forall t > 0: \quad \nu_{\mathcal{F}}(x_*, t) := \inf\{\mathcal{B}_{\mathcal{F}}(x_*, x) \mid x \in \mathbb{X} \wedge \|x - x_*\|_{\mathbb{X}} = t\}. \quad (2.4)$$

The functional  $\mathcal{F}$  is called *totally nonlinear* at  $x_*$ , if  $\nu_{\mathcal{F}}(x_*, t) > 0$  for all  $t \in (0, \infty)$ .

According to [35],  $\mathcal{F}$  is totally nonlinear at  $x_* \in \mathbb{X}$  if and only if for all bounded sequences  $(x_n)_{n \in \mathbb{N}} \in \mathbb{X}^{\mathbb{N}}$  with  $\lim_{n \rightarrow \infty} \mathcal{B}_{\mathcal{F}}(x_*, x_n) = 0$  we have  $\lim_{n \rightarrow \infty} \|x_n - x_*\|_{\mathbb{X}} = 0$ .

**Theorem 2.6** (Stong convergence). *In the situation of Theorem 2.4 assume additionally that the  $\mathcal{R}$ -minimizing solution  $x^+$  of  $\mathbf{A}x = y$  is unique and that  $\mathcal{R}$  is totally nonlinear at  $x^+$ . Then,  $\|x_n - x^+\|_{\mathbb{X}} \rightarrow 0$  as  $n \rightarrow \infty$ .*

*Proof.* According to Theorem 2.4, the sequence  $(x_n)_{n \in \mathbb{N}}$  converges weakly to  $x^+$  and  $\mathcal{R}(x^+) = \lim_{n \rightarrow \infty} \mathcal{R}(x_n)$ . Because  $\mathcal{R}'(x^+)$  is bounded,  $\mathcal{R}'(x^+)(x_n - x^+) \rightarrow 0$  and thus  $\mathcal{B}_{\mathcal{R}}(x^+, x_n) = |\mathcal{R}(x_n) - \mathcal{R}(x^+) - \mathcal{R}'(x^+)(x_n - x^+)| \rightarrow 0$ . Because  $(x_n)_{n \in \mathbb{N}}$  is bounded with the total nonlinearity of  $\mathcal{R}$  this yields  $x_n \rightarrow x^+$ .  $\square$

## 2.2 Training strategy

Given a sequence of noise levels  $(\delta_n)_{n \in \mathbb{N}}$ , our aim is to construct the data-driven regularizer  $\|\Phi_n(x) - x\|^2/2$  with neural networks  $\Phi_n$  adapted to training signals  $x_i \in \mathbb{X}$  for  $i \in I :=$

$\{1, \dots, N\}$  that we consider as ground truth and corresponding perturbed signals  $x_i + r_{i,n,j} \in \mathbb{X}$  for  $j \in J_{i,n}$  that we want to avoid. Given a family  $(\Phi_\theta)_{\theta \in \Theta}$ , we determine the parameter  $\theta = \theta_n$  as the minimizer of

$$\mathcal{L}_n(\theta) := \sum_{i \in I} \sum_{j \in J_{i,n}^*} \|\Phi_\theta(x_i + r_{i,n,j}) - x_i\|^2, \quad (2.5)$$

where  $J_{i,n}^* := J_{i,n} \cup \{0\}$  and  $r_{i,n,0} := 0$  for the ground truth signals. Notice that the index  $i$  indicates the training example, the index  $n$  the noise level, and the index  $j$  refers to the perturbations for a given training example and noise level.

By doing so, we have  $(\Phi_n - \text{Id})(x_i) \simeq 0$  for the ground truth signals  $x_i$  and  $(\Phi_n - \text{Id})(x_i + r_{i,n,j}) \simeq r_{i,n,j}$  for the perturbed signals  $x_i + r_{i,n,j}$ . Hence the regularizer  $\|(\Phi_n - \text{Id})(\cdot)\|$  is expected to be small for signals similar to  $x_i$  and large for signals similar to  $x_i + r_{i,n,j}$ . A specific feature of our learned regularizer is that it can depend on the forward problem. This is achieved by making the perturbations  $r_{i,n,j}$  operator specific. A strategy for increasing this dependence is to let the architecture depend on  $\mathbf{A}$  such as a null space network [51] or data-proximal network [18].

**Remark 2.7** (Choice of the perturbations). *A crucial question is how to construct proper perturbed signals  $x_i + r_{i,n,j} \in \mathbb{X}$  for  $j \neq 0$ . For NETT, we proposed in [35] to choose a single perturbation  $r_{i,n,1} = r_i^* := (\text{Id} - \mathbf{A}^+ \mathbf{A})(x_i) \in \ker(\mathbf{A})$  per training example, which is also independent of the noise. This choice is well suited to address non-uniqueness, a primary issue in undersampled tomographic inverse problems where the kernel  $\ker(\mathbf{A})$  has high dimensionality. In this work, we are also concerned with ill-posed and ill-conditioned problems where small singular values pose an additional challenge, alongside the possibly large kernel. As a result, we modify the training strategy of [35] by introducing multiple perturbations  $r_{i,n,j}$  that address two additional factors: some perturbations represent noise in the low-frequency components corresponding to large singular values, while others reflect damped high-frequency components of the signal corresponding to small or vanishing singular values.*

Let  $(u_n, v_n, \sigma_n)_{n \in \mathbb{N}}$  denote a singular value decomposition (SVD) of  $\mathbf{A}$ . We allow the operator  $\mathbf{A}$  to have a nontrivial kernel  $\ker(\mathbf{A}) \neq \{0\}$  and a non-dense range  $\overline{\text{ran}(\mathbf{A})} \neq \mathbb{Y}$ , and we only include the non-vanishing singular values in the definition of  $\sigma_n$ . In such a situation we can express  $\mathbf{A}$ , its pseudoinverse, and the truncated SVD reconstruction by the formulas

$$\begin{aligned} \mathbf{A}(x) &= \sum_{n \in \mathbb{N}} \sigma_n \langle x, u_n \rangle v_n \\ \mathbf{A}^+(y) &= \sum_{n \in \mathbb{N}} \sigma_n^{-1} \langle y, v_n \rangle u_n \\ \mathbf{S}_\alpha(y) &= \sum_{\sigma_n^2 \geq \alpha} \sigma_n^{-1} \langle y, v_n \rangle u_n, \end{aligned}$$



where  $\alpha \geq 0$  is the regularization parameter.

Now if  $x_i$  is a given ground truth signal and  $y_{i,n} = \mathbf{A}x_i + z_{i,n}$  corresponding noisy data, and  $\alpha[n, j]$  for  $j \in J_n$  are variable chosen regularization parameters in truncated SVD, we consider perturbed signals

$$x_i + r_{i,n,j} := \mathbf{S}_{\alpha[n,j]}(\mathbf{A}x_i + z_{i,n}).$$

In fact, the perturbed signals are truncated SVD regularized reconstructions with perturbations  $r_{i,n,j} = \mathbf{S}_{\alpha[n,j]}(\mathbf{A}x_i + z_{i,n}) - x_i$ . In particular, for  $z_{i,n} = 0$  and  $\alpha[n, 1] = 0$ , we recover the perturbations  $r_i^* = \mathbf{A}^+ \mathbf{A}x_i - x_i$  proposed in [35] for NETT, which can be seen as pure artifacts (meaning elements in the null space caused by projecting  $x_i$  onto  $\ker(\mathbf{A})^\perp$ ). The more general strategy that is proposed here also includes perturbations due to noise and to Gibbs-type artifacts caused by truncation of singular components.

### 3 Application

In this section, we present numerical results for an inverse problem in attenuation correction in photoacoustic tomography (PAT), as described in more detail below. We consider a discrete setting where the operator  $\mathbf{A} \in \mathbb{R}^{d \times d}$  is a matrix of size  $d = 601$  and  $x \in \mathbb{R}^d$  is the time discretization of a real-valued function defined on the interval  $[0, T]$ . The additional regularizer  $\mathcal{Q}$  is taken either as zero or as the total variation (TV). Details on the forward operator, the learned regularizer, and the numerical solution of (2.1) are given below.

#### 3.1 Attenuation correction in PAT using the NSW model

The problem we have selected for testing the learned Morozov regularization is attenuation correction in PAT. The corresponding forward operator has a significant number of large and small singular values, making appropriate regularization highly important. It is 1D and thus numerically efficient and of non-convolutional form, ensuring it is not too simplistic to draw conclusions from. Finally, it is of practical significance, as 1D attenuation correction can serve as a module for two- and three-dimensional image reconstruction, as we argue below.

**PAT in attenuating media:** PAT is a hybrid imaging technology based on the conversion of optical energy into acoustic pressure waves, and combines the high spatial resolution of ultrasound imaging with the high contrast of optical imaging. A general model for PAT in attenuating media is (see [30, 31])

$$\left( \mathbf{D}_\alpha + \frac{1}{c_0} \frac{\partial}{\partial t} \right)^2 p_\alpha(x, t) - \Delta p_\alpha(x, t) = \delta'(t)h(x) \quad \text{for } (x, t) \in \mathbb{R}^D \times \mathbb{R}. \quad (3.1)$$

Here  $D \in \{1, 2, 3\}$  is the spatial dimension,  $h: \mathbb{R}^D \rightarrow \mathbb{R}$  is the photoacoustic (PA) source,  $c_0 > 0$  is a constant, and  $\mathbf{D}_\alpha$  is the time convolution operator associated with the inverse Fourier transform of the complex valued attenuation function  $\alpha: \mathbb{R} \rightarrow \mathbb{C}$ . The image reconstruction problem associated to (3.1) consists in reconstructing the source  $h$  from measurements of  $p_\alpha$  recorded at detector positions  $x$  on an  $(D - 1)$ -dimensional manifold. The case  $\alpha = 0$  corresponds to absence of attenuation where several efficient and accurate inversion methods exist including explicit inversion formulas [16, 17, 24, 32, 40, 43, 54] or iterative approaches [4, 7, 11, 23, 25, 44, 47].

**The NSW model:** A variety of attenuation models exist, depending on the form of the complex-valued function  $\alpha$ ; causal models are of particular interest [30, 31]. In this paper, we work with the causal model of Nachman, Smith, and Waag (NSW model) with a single relaxation process [39], for which the complex attenuation function takes the form

$$\alpha(\omega) = \frac{(-i\omega)}{c_\infty} \left( \frac{c_\infty}{c_0} \sqrt{\frac{1 + (c_0/c_\infty)^2 (-i\tau_1\omega)}{1 + (-i\tau_1\omega)}} - 1 \right), \quad (3.2)$$

with parameters  $c_0, \tau_1, c_\infty$ . Equation (3.2) and its generalization using  $N$  relaxation processes have been derived in [39] based on sound physical principles.

**Attenuation correction:** According to [29, Theorem 1 and Lemma 1], the attenuated pressure signals can be expressed in terms of the unattenuated ones by

$$p_\alpha(x, t) = \int_0^t m_\alpha(t, r) p_0(x, r) dr, \quad (3.3)$$

$$\mathcal{F}(m_\alpha(\cdot, r))(\omega) = \frac{\omega}{\omega/c_0 + i\alpha(\omega)} e^{i(\omega/c_0 + i\alpha(\omega))|r|}, \quad (3.4)$$

for  $r, t > 0$ ,  $\omega \in \mathbb{R}$  and  $x \in \mathbb{R}^D$ . Here,  $p_\alpha$  and  $p_0$  denote the causal solutions of (3.1) with and without attenuation, respectively, and  $\mathcal{F}$  is the Fourier transform in the first argument. This shows that the PA source  $h$  can be recovered by first solving the 1D reconstruction problem (3.3) for  $p_0$  and then recovering  $h$  from the estimated unattenuated signals. Such a two-step method has been proposed and implemented for the power law in [33, 34], and later used in [2, 31] for various attenuation laws. We refer to the inversion of (3.3) as 1D attenuation correction.

**Note on the ill-posedness:** The analysis of [14] on the singular values of PAT in attenuating media shows that reconstructing  $h$  based on the NSW model shares the same asymptotic behavior of singular values as the inversion problem in PAT without attenuation. Consequently, in the continuous setting, the 1D attenuation correction problem defined by (3.3) is

expected to be stable. However, the singular values are predicted to decay rapidly at first, as the attenuation of a pressure-emitting source increases with both  $\omega$  and the distance from the observer. The singular value plot for the discretized operator in Figure 1 confirms this expectation and demonstrates that the discrete problem is ill-conditioned.

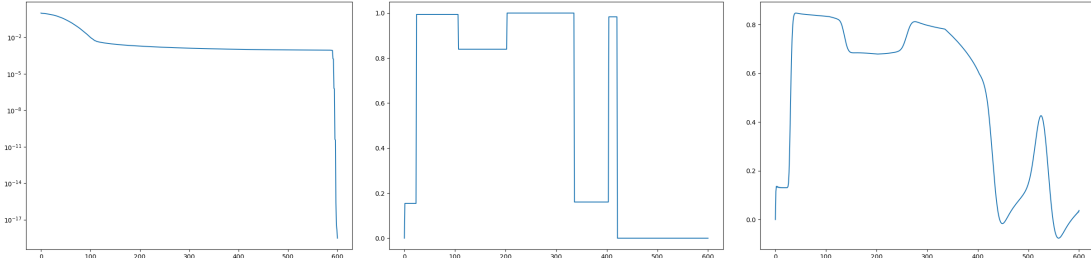


Figure 1: Left: Singular values of the  $\mathbf{A} \in \mathbb{R}^{d \times d}$  modeling dissipation on a logarithmic scale. Middle: Test signal  $x \in \mathbb{R}^d$ . Right: Exact data  $\mathbf{A}x$  for input from the middle picture. The horizontal axis in the middle and right images represents time.

### 3.2 Implementation details

**Forward operator:** The forward operator  $\mathbf{A}$  is taken as a discretization of the 1D integral operator defined by (3.3) that maps unattenuated pressure signals to attenuated signals. We use the NSW model (3.2) with parameters  $c_0 = 1$ ,  $\tau_1 = 10^{-4}$ , and  $c_\infty = 1.41$  calculated over the temporal interval  $[0, 0.1]$ . Its operation is illustrated in Figure 1 (center and right). For details on how the matrix  $\mathbf{A}$  was computed, see [21]. Due to the fast decay of the singular values of  $\mathbf{A}$  (Figure 1, left), the solution of (1.1) in this case is severely ill-conditioned. Moreover, the operator is not of convolutional form, and the ill-conditioning increases for signal components corresponding to later times. This can be seen in the right image in Figure 1, where the right part of the signal is significantly more blurred than the left.

**Network architecture:** As the network architecture  $(\Phi_\theta)_{\theta \in \Theta}$ , we utilize a one-dimensional version of the 2D U-Net [46] with skip connection. The architecture begins with several convolutional blocks, each consisting of two 1D convolutional layers with ELU activation, where the number of filters doubles at each block, starting from 16. Downsampling is achieved using strided convolutions, which halve the spatial size of the feature maps at each stage. Upon reaching the bottleneck, the network employs transposed convolutions (upsampling) to restore the original spatial size. Skip connections between corresponding layers in the encoder and decoder paths are incorporated to retain detailed features. The final output is generated through a concluding convolutional layer, with the option to either add the input signal to the output (thus learning the residuals) or produce the entire signal directly without this addition.

Dropout layers are integrated to prevent overfitting and enhance generalization. The design is intentionally kept simple to minimize computational time, as developing a sophisticated network architecture is not the primary focus of this work.

**Network training:** For the training signals  $x_i$ , we utilize a collection of block signals similar to those in [13]. We scale the input signals  $x_i$  to have a maximum value of 1 and construct noisy data as  $\mathbf{A}x_i + z_{i,n}$ , where  $z_{i,n}$  is normally distributed noise with mean zero and standard deviation proportional to  $\sigma$  and the mean value of  $\mathbf{A}x_i$ . The full training dataset consists of 5000 ground truth signals  $x_i$  and 5000 perturbed signals for each  $n$  and each  $\alpha[n, j] = j/10$  with  $j \in \{1, \dots, 8\}$ . According to Section 2.2, the network is trained by minimizing the risk  $\mathcal{L}_n(\theta) = \sum_i \sum_j \|\Phi_\theta(x_i + r_{i,n,j}) - x_i\|^2$ . The trained network is then denoted as  $\Phi_n := \Phi_{\theta_n}$ , where  $\theta_n$  is the numerical minimizer of  $\mathcal{L}_n$ .

**Numerical Morozov regularization:** Reconstruction is done by numerically solving (2.1) with the noise-adaptive data-driven regularizer  $\mathcal{R}_n := \|(\text{Id} - \Phi_n)(\cdot)\|^2/2 + \|\mathbf{L}x\|_1$ , where  $\|\cdot\|_1$  is the  $\ell^1$ -norm and  $\mathbf{L}$  is either zero (no additional regularizer) or taken as the discrete central difference operator with Neumann boundary conditions (TV as additional regularizer). For computing numerical solutions we write (2.1) in the form

$$\min_x \|\Phi_n(x) - x\|_2^2 + \lambda \|\mathbf{L}x\|_1 + \mathbf{1}_B(\mathbf{A}x) \quad (3.5)$$

with  $\mathbf{1}_B$  denoting the indicator function of  $B = \{y \in \mathbb{R}^d \mid \|y - y_\delta\| \leq \delta\}$ . Optimization problem (3.5) is then solved using the primal dual algorithm of [10]. With the abbreviations  $f(x) := \|\Phi_n(x) - x\|_2^2$ ,  $h_1 := \lambda \|\cdot\|_1$  and  $h_2 := \mathbf{1}_B$ , parameters  $\tau, \sigma, \rho > 0$  and initial values  $x^{(0)}$  and  $y^{(0)} = (0, 0)$  the proposed reconstruction algorithm reads

$$\begin{aligned} z^{(i+1)} &:= x^{(i)} - \tau \nabla f(x^{(i)}) - \tau \mathbf{L}^* y_1^{(i)} - \tau \mathbf{A}^* y_2^{(i)} \\ x^{(i+1)} &:= \rho z^{(i+1)} + (1 - \rho)x^{(i)} \\ w_1^{(i+1)} &:= \text{prox}_{\sigma h_1^*}(y_1^{(i)} + \sigma \mathbf{L}(2z^{(i+1)} - x^{(i)})) \\ y_1^{(i+1)} &:= \rho w_1^{(i+1)} + (1 - \rho)y_1^{(i)} \\ w_2^{(i+1)} &:= \text{prox}_{\sigma h_2^*}(y_2^{(i)} + \sigma \mathbf{A}(2z^{(i+1)} - x^{(i)})) \\ y_2^{(i+1)} &:= \rho w_2^{(i+1)} + (1 - \rho)y_2^{(i)}. \end{aligned}$$

Here prox denotes the proximity mapping and  $(\cdot)^*$  the Fenchel dual. The proximity mappings  $\text{prox}_{\sigma h_1^*}$ ,  $\text{prox}_{\sigma h_2^*}$  can be easily computed using the relation  $\text{prox}_{h^*} + \text{prox}_h = \text{Id}$  and the known expressions for the proximity mappings of  $\|\cdot\|_1$  and  $\mathbf{1}_B$ . When  $\mathbf{L} = 0$ , the iterative algorithm does not require the  $y_1$  and  $w_1$  updates.

Concerning the convergence of the algorithm, we note that for a linear network  $\Phi_n$ , the functional  $f$  is convex, and the convergence analysis of [10, Theorem 3.3] can be applied, guaranteeing the convergence of the sequence  $(x^{(i)}, y^{(i)})_{i \in \mathbb{N}}$ . In the general and important case of a non-convex network regularizer, we are not aware of theoretical results that assure the proposed algorithm’s convergence. Results similar to those in [53], obtained for a related algorithm, seem possible and would be an interesting line of research.

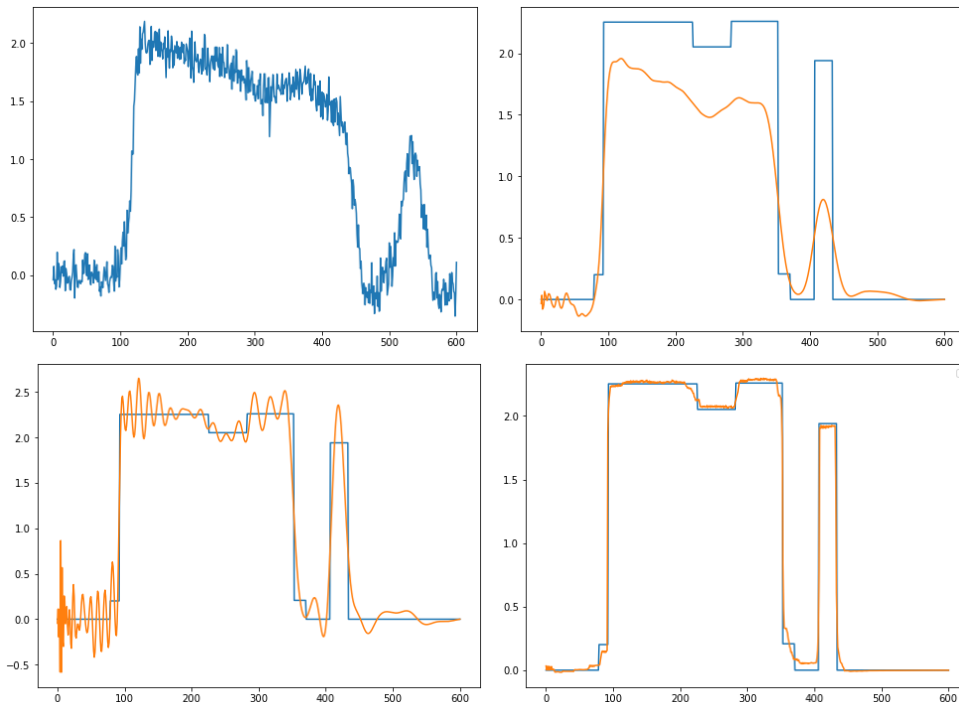


Figure 2: Top left: Noisy data  $y_\delta$ . Top right: BP reconstruction. Bottom left: SVD reconstruction. Bottom right: DD-Morozov regularization .

**Tikhonov regularization:** In the results section, we will compare the Morozov-type regularizations with their Tikhonov counterparts, which minimize the Tikhonov functional

$$\mathcal{T}_{\alpha, y_\delta}(x) := \frac{1}{2} \|\mathbf{A}x - y_\delta\|_2^2 + \alpha \|\Phi_n(x) - x\|_2^2 + \lambda \|\mathbf{L}x\|_1. \quad (3.6)$$

The case  $\alpha = 0$  corresponds to standard TV-regularization [1], and the case  $\lambda = 0$  corresponds to NETT (network Tikhonov) regularization [35]. Additionally, we present results for the mixed case where both regularizers are active. Minimization of all NETT variants is performed using incremental gradient descent.

### 3.3 Results

**Proof of concept:** Figure 2 shows results for a randomly selected block signal  $x$ , which is not part of the training data. The upper left image displays the noisy attenuated signal  $y_\delta$ , while the upper right image shows the backprojection (BP) reconstruction  $\mathbf{A}^T y_\delta$ . The lower left image illustrates the truncated SVD reconstruction  $\mathbf{S}_\alpha y_\delta$  with  $\alpha = 0.1$ , and the lower right image shows the results using the proposed DD-Morozov regularization with TV as an additional regularizer. The BP reconstruction is noticeably damped, whereas the SVD reconstruction exhibits strong oscillations. The DD-Morozov regularization, as shown by applying methods (1.3) and (2.1), is clearly superior. Similar results have been achieved for other randomly selected test signals.

	TV	CNN	TV plus CNN
$\ell^2$ errors using CNN initialization			
Tikhonov	$0.0866 \pm 0.045$	$0.0874 \pm 0.045$	$0.0866 \pm 0.045$
Morozov	$0.0877 \pm 0.046$	$0.0872 \pm 0.045$	$0.0866 \pm 0.044$
$\ell^2$ errors using zero initialization			
Tikhonov	$0.100 \pm 0.032$	$0.107 \pm 0.032$	$0.100 \pm 0.039$
Morozov	$0.090 \pm 0.034$	$0.108 \pm 0.033$	$0.103 \pm 0.033$

Table 1: Comparison of various variants of Morozov regularization with variants of Tikhonov regularization. CNN-Tikhonov is the NETT and TV-Tikhonov is standard TV-regularization. Mean and standard deviation of the  $\ell^2$  reconstruction errors have been computed for 500 samples with  $\delta = 0.1$ .

**Comparison with NETT and TV regularization:** While the results shown in Figure 2 demonstrate that DD-Morozov regularization improves reconstructions compared to very simple regularization methods, we next evaluate DD-Morozov regularization with TV as an additional regularizer against DD-Morozov regularization without additional regularization, Morozov with TV, as well as their counterparts minimizing the Tikhonov functional (3.6). For all methods, we evaluated performance using either an initial estimate from the neural network prediction with truncated SVD as input or zero initialization. The results shown in Table 1 clearly demonstrate that the network initialization consistently outperforms zero initialization. Additionally, all methods with truncated SVD initialization reduced the mean error  $0.089 \pm 0.046$  of the initial guess. The TV-Tikhonov method performed similarly to NETT and NET-Morozov. Figure 3 illustrates a representative example of signal reconstruction, where the proposed method with TV regularization strikes a good balance between smoothing the signal and preserving fine details.

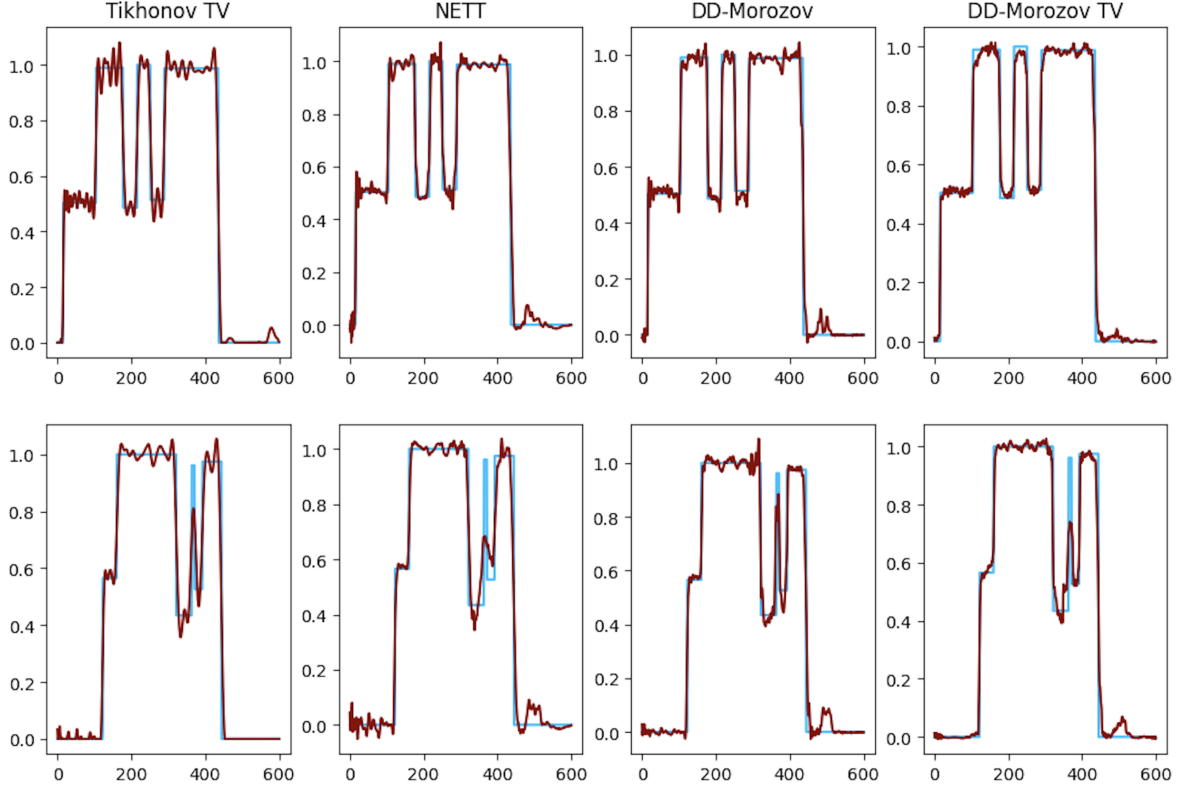


Figure 3: Comparison of several methods using either the network output (top) or the zero signal as initial guess (bottom). The columns from left to right show Tikhonov regularization with TV as the regularizer, the NETT, DD-Morozov without TV, and DD-Morozov with TV as an additional regularizer. For the network as initial guess, the truncated SVD reconstruction applied to noisy data has been used as input for the neural network that has been trained for the regularizer.

**Numerical convergence:** To illustrate the convergence stated in Theorem 2.4, we performed numerical simulations under decreasing noise levels. Specifically, we trained six different networks, each exposed to a separate noise level with  $\sigma \in \{0.005, 0.01, 0.05, 0.1, 0.15, 0.2\}$ . We analyzed the method’s average performance across 500 additional samples while progressively decreasing the noise levels. Our empirical results, shown in Figure 4, indicate that as the noise levels decrease, the method’s performance improves, thus providing empirical support for the theoretical convergence result presented in Theorem 2.4.

**Influence of correct noise level:** Our proposed training strategy requires an assumed noise level. To assess the sensitivity of the trained networks to variations in this levels, we conducted experiments comparing the performance of networks trained at noise levels of 0.01 and 0.2 when evaluated on a test dataset with a noise level of 0.1. The results are shown in Table 2. We observe that training the networks with incorrect noise levels leads to a slight

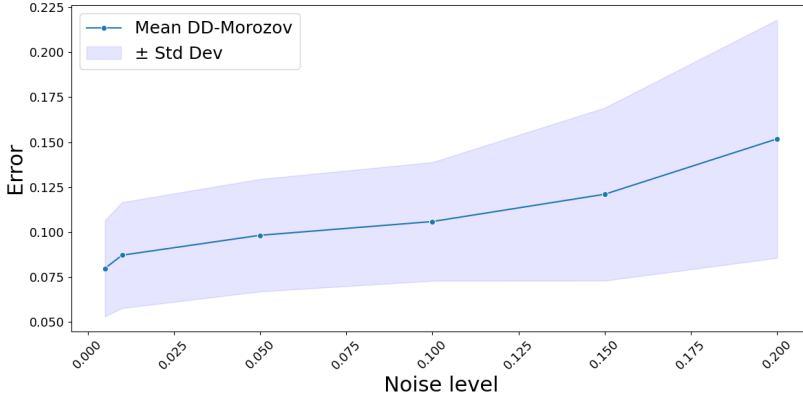


Figure 4: Mean value and standard deviation of the  $\ell^2$  reconstruction error as a function of the noise level  $\delta$ .

decrease in performance. However, the results appear relatively stable, even when the wrong noise level is used for training.

Noise level in training	Average $\pm$ standard deviation of $\ell^2$ -error
0.10 (correct)	$0.110 \pm 0.033$
0.01 (underestimated)	$0.114 \pm 0.033$
0.20 (overestimated)	$0.112 \pm 0.032$

Table 2: Average reconstruction error and standard deviation of DD-Morozov regularization on the dataset with noise level 0.1 using networks trained on correct (top) underestimated (middle; trained with 0.01) and overestimated (bottom; trained with 0.2) noise level.

**Theory versus numerics:** The weak convergence result from Theorem 2.4 relies on networks that satisfy the conditions of Assumption 2.1, which appear to be quite natural. Due to the architectural choices, the networks  $\Phi$  and  $\Phi_{\theta(\delta)}$  are Lipschitz continuous, fulfilling (A1). Assumptions (A2) and (A3) are conditions on the convergence of  $\Phi_{\theta(\delta)}$  to some network  $\Phi$  as  $\delta \rightarrow 0$ . Since we use the same architecture and apply perturbations that diminish with decreasing noise levels this behavior is anticipated in our case; a rigorous proof however still requires careful adjustments to the loss function and proper initialization. This could be an interesting direction for future research, particularly as it applies to trained regularizers in general. Considering that the simulations are carried out in a finite-dimensional, ill-conditioned setting, strong convergence is already implied by weak convergence. However, ensuring that convergence is independent of the discretization requires total convexity (see Theorem 2.6). In a broader context, a trained regularizer may not always satisfy this assumption. Determining how to guarantee this during training presents another interesting topic for future research.



## 4 Summary

In this paper, we introduced and analyzed neural network-based noise-adaptive Morozov regularization using a data-driven regularizer (NN-Morozov regularization). We performed a complete convergence analysis that also allows for noise-dependent regularizers. In addition, we established convergence in strong topology. To make our approach practical, we developed a simple yet efficient training strategy extending NETT [35]. We verified our methodology through numerical experiments, with a special focus on its application to attenuation correction for PAT. Our research can provide the basis for a broader integration of data-driven regularizers into various variational regularization techniques.

## References

- [1] R. Acar and C. R. Vogel. Analysis of bounded variation penalty methods for ill-posed problems. *Inverse problems*, 10(6):1217, 1994.
- [2] H. Ammari, E. Bretin, V. Jugnon, and A. Wahab. Photoacoustic imaging for attenuating acoustic media. In *Mathematical modeling in biomedical imaging II*, pages 57–84. Springer, 2012.
- [3] S. Arridge, P. Maass, O. Öktem, and C.-B. Schönlieb. Solving inverse problems using data-driven models. *Acta Numerica*, 28:1–174, 2019.
- [4] S. R. Arridge, M. M. Betcke, B. T. Cox, F. Lucka, and B. E. Treeby. On the adjoint operator in photoacoustic tomography. *Inverse Probl.*, 32(11):115012 (19pp), 2016.
- [5] A. Aspri, S. Banert, O. Öktem, and O. Scherzer. A data-driven iteratively regularized Landweber iteration. *Numerical Functional Analysis and Optimization*, 41(10):1190–1227, 2020.
- [6] A. Aspri, Y. Korolev, and O. Scherzer. Data driven regularization by projection. *Inverse Problems*, 36(12):125009, 2020.
- [7] Z. Belhachmi, T. Glatz, and O. Scherzer. A direct method for photoacoustic tomography with inhomogeneous sound speed. *Inverse Probl.*, 32(4):045005, 2016.
- [8] M. Benning and M. Burger. Modern regularization methods for inverse problems. *Acta numerica*, 27:1–111, 2018.
- [9] P. Blanchard and E. Brüning. *Variational Methods in Mathematical Physics. A Unified Approach*. Springer-Verlag, Berlin, 1992.

- [10] L. Condat. A primal–dual splitting method for convex optimization involving lipschitzian, proximable and linear composite terms. *Journal of optimization theory and applications*, 158(2):460–479, 2013.
- [11] X. L. Dean-Ben, A. Buehler, V. Ntziachristos, and D. Razansky. Accurate model-based reconstruction algorithm for three-dimensional optoacoustic tomography. *IEEE Trans. Med. Imag.*, 31(10):1922–1928, 2012.
- [12] S. Dittmer, T. Kluth, P. Maass, and D. Otero Baguer. Regularization by architecture: A deep prior approach for inverse problems. *Journal of Mathematical Imaging and Vision*, 62:456–470, 2020.
- [13] D. L. Donoho and I. M. Johnstone. Ideal spatial adaptation by wavelet shrinkage. *Biometrika*, 81:425–455, 1994.
- [14] P. Elbau, O. Scherzer, and C. Shi. Singular values of the attenuated photoacoustic imaging operator. *Journal of Differential Equations*, 263(9):5330–5376, 2017.
- [15] H. W. Engl, M. Hanke, and A. Neubauer. *Regularization of inverse problems*, volume 375. Kluwer Academic Publishers Group, Dordrecht, 1996.
- [16] D. Finch, M. Haltmeier, and Rakesh. Inversion of spherical means and the wave equation in even dimensions. *SIAM J. Appl. Math.*, 68(2):392–412, 2007.
- [17] D. Finch, S. K. Patch, and Rakesh. Determining a function from its mean values over a family of spheres. *SIAM J. Math. Anal.*, 35(5):1213–1240, 2004.
- [18] S. Göppel, J. Friel, and M. Haltmeier. Data-proximal null-space networks for inverse problems. *arXiv:2309.06573*, 2023.
- [19] A. Goujon, S. Neumayer, P. Bohra, S. Ducotterd, and M. Unser. A neural-network-based convex regularizer for inverse problems. *IEEE Transactions on Computational Imaging*, 2023.
- [20] M. Grasmair, M. Haltmeier, and O. Scherzer. The residual method for regularizing ill-posed problems. *Applied Mathematics and Computation*, 218(6):2693–2710, 2011.
- [21] M. Haltmeier, R. Kowar, and L. V. Nguyen. Iterative methods for pat in attenuating acoustic media. *Inverse Problems 33 (11)*, 2017.
- [22] M. Haltmeier and L. Nguyen. Regularization of inverse problems by neural networks. In K. Chen, C.-B. Schönlieb, X.-C. Tai, and L. Younces, editors, *Handbook of Mathematical Models and Algorithms in Computer Vision and Imaging: Mathematical Imaging and Vision*, pages 1–29. Springer International Publishing, Cham, 2021.

- [23] M. Haltmeier and L. V. Nguyen. Analysis of iterative methods in photoacoustic tomography with variable sound speed. *SIAM Journal on Imaging Sciences*, 10(2):751–781, 2017.
- [24] M. Haltmeier and S. Pereverzyev Jr. The universal back-projection formula for spherical means and the wave equation on certain quadric hypersurfaces. *J. Math. Anal. Appl.*, 429(1):366–382, 2015.
- [25] C. Huang, K. Wang, L. Nie, L. V. Wang, and M. A. Anastasio. Full-wave iterative image reconstruction in photoacoustic tomography with acoustically inhomogeneous media. *IEEE transactions on medical imaging*, 32(6):1097–1110, 2013.
- [26] K. Ito and B. Jin. *Inverse problems: Tikhonov theory and algorithms*, volume 22. World Scientific, 2014.
- [27] V. K. Ivanov, V. V. Vasin, and V. P. Tanana. *Theory of linear ill-posed problems and its applications*, volume 36. Walter de Gruyter, 2013.
- [28] E. Kobler, A. Effland, K. Kunisch, and T. Pock. Total deep variation for linear inverse problems. In *Proceedings of the IEEE/CVF Conference on computer vision and pattern recognition*, pages 7549–7558, 2020.
- [29] R. Kowar. Integral equation models for thermoacoustic imaging of acoustic dissipative tissue. *Inverse Probl.*, 26(9):095005, 2010.
- [30] R. Kowar and O. Scherzer. Attenuation models in photoacoustics. In *Mathematical modeling in biomedical imaging II: Optical, ultrasound, and opto-acoustic tomographies*, pages 85–130. Springer, 2011.
- [31] R. Kowar and O. Scherzer. Photoacoustic imaging taking into account attenuation. In *Mathematics and Algorithms in Tomography*, volume 18, pages 54–56. Springer, 2012.
- [32] L. A. Kunyansky. Explicit inversion formulae for the spherical mean Radon transform. *Inverse Probl.*, 23(1):373–383, 2007.
- [33] P. J. La Riviere, J. Zhang, and M. A. Anastasio. Image reconstruction in optoacoustic tomography accounting for frequency-dependent attenuation. *Nuclear Science Symposium Conference Record, 2005 IEEE*, 4:5 pp., 2005.
- [34] P. J. La Rivière, J. Zhang, and M. A. Anastasio. Image reconstruction in optoacoustic tomography for dispersive acoustic media. *Opt. Lett.*, 31(6):781–783, 2006.
- [35] H. Li, J. Schwab, S. Antholzer, and M. Haltmeier. NETT: Solving inverse problems with deep neural networks. *Inverse Problems*, 36(6):065005, 2020.

- [36] S. Lutz, O. Öktem, and C.-B. Schönlieb. Adversarial regularizers in inverse problems. *Advances in neural information processing systems*, 31, 2018.
- [37] V. A. Morozov. *Regularization Methods for Ill-Posed Problems*. CRC Press, Boca Raton, 1993.
- [38] S. Mukherjee, M. Carioni, O. Öktem, and C.-B. Schönlieb. End-to-end reconstruction meets data-driven regularization for inverse problems. *Advances in neural information processing systems*, 34:21413–21425, 2021.
- [39] A. I. Nachman, J. F. Smith III, and R. C. Waag. An equation for acoustic propagation in inhomogeneous media with relaxation losses. *J. Acoust. Soc. Am.*, 88(3):1584–1595, 1990.
- [40] F. Natterer. Photo-acoustic inversion in convex domains. *Inverse Problems Imaging*, 2012.
- [41] F. Natterer and F. Wübbeling. *Mathematical Methods in Image Reconstruction*, volume 5 of *Monographs on Mathematical Modeling and Computation*. SIAM, Philadelphia, PA, 2001.
- [42] D. Obmann, L. Nguyen, J. Schwab, and M. Haltmeier. Augmented NETT regularization of inverse problems. *Journal of Physics Communications*, 5(10):105002, 2021.
- [43] V. P. Palamodov. A uniform reconstruction formula in integral geometry. *Inverse Probl.*, 28(6):065014, 2012.
- [44] G. Paltauf, J. A. Viator, S. A. Prahl, and S. L. Jacques. Iterative reconstruction algorithm for optoacoustic imaging. *J. Opt. Soc. Am.*, 112(4):1536–1544, 2002.
- [45] D. Riccio, M. J. Ehrhardt, and M. Benning. Regularization of inverse problems: Deep equilibrium models versus bilevel learning. *arXiv:2206.13193*, 2022.
- [46] O. Ronneberger, P. Fischer, and T. Brox. U-net: Convolutional networks for biomedical image segmentation. In *Medical Image Computing and Computer-Assisted Intervention—MICCAI 2015: 18th International Conference, Munich, Germany, October 5–9, 2015, Proceedings, Part III 18*, pages 234–241. Springer, 2015.
- [47] A. Rosenthal, V. Ntziachristos, and D. Razansky. Acoustic inversion in optoacoustic tomography: A review. *Current medical imaging reviews*, 9(4):318, 2013.
- [48] S. Roth and M. J. Black. Fields of experts: A framework for learning image priors. In *2005 IEEE Computer Society Conference on Computer Vision and Pattern Recognition (CVPR’05)*, volume 2, pages 860–867. IEEE, 2005.

- [49] O. Scherzer, M. Grasmair, H. Grossauer, M. Haltmeier, and F. Lenzen. *Variational methods in imaging*, volume 167 of *Applied Mathematical Sciences*. Springer, New York, 2009.
- [50] T. Schuster, B. Kaltenbacher, B. Hofmann, and K. S. Kazimierski. *Regularization methods in Banach spaces*, volume 10. Walter de Gruyter, 2012.
- [51] J. Schwab, S. Antholzer, and M. Haltmeier. Deep null space learning for inverse problems: convergence analysis and rates. *Inverse Problems*, 35(2):025008, 2019.
- [52] A. N. Tikhonov and V. Arsenin. *Solutions of ill-posed problems*. John Wiley & Sons, Washington, D.C., 1977.
- [53] T. Valkonen. A primal–dual hybrid gradient method for nonlinear operators with applications to mri. *Inverse Problems*, 30(5):055012, 2014.
- [54] M. Xu and L. V. Wang. Universal back-projection algorithm for photoacoustic computed tomography. *Phys. Rev. E*, 71(1):016706, 2005.